INTERNATIONAL ATOMIC ENERGY AGENCY
UNITED NATIONS EDUCATIONAL, SCIENTIFIC AND CULTURAL ORGANIZATION
INTERNATIONAL CENTRE FOR THEORETICAL PHYSICS
I.C.T.P., P.O. BOX 586, 34100 TRIESTE, ITALY, CABLE: CENTRATOM TRIESTE

H4.SMR/709-4

Second Workshop on Non-Linear Dynamics
and Earthquake Prediction

22 November - 10 December 1993

V_p/V_s Estimation in Southwestern Europe from P-wave and Surface-Wave Tomography Analysis

[1], [2], [3] F. Vaccari, [1], [3] G. F. Panza

[1] Istituto di Geodesia e Geofisica
Università di Trieste,
Trieste, Italy

[2] CNR, Gruppo Nazionale per la Difesa dai Terremoti
Roma, Italy

[3] International Center for Theoretical Physics
Trieste, Italy

Physics of the Earth and Planetary Interiors, 78 (1993) 229–237
Elsevier Science Publishers B.V., Amsterdam

V_P/V_S estimation in southwestern Europe from P-wave and surface-wave tomography analysis

F. Vaccari [*,a,b,c], G.F. Panza [a,c]

[a] *Istituto di Geodesia e Geofisica, Universitá di Trieste, Via dell'Università 7, T-34123, Trieste, Italy*
[b] *CNR, Gruppo Nazionale per la Difesa dai Terremoti, Via Nizza 128, I-00198, Roma, Italy*
[c] *International Center for Theoretical Physics, P.O. Box 586, I-34100, Trieste, Italy*

(Received 10 February 1992; revision accepted 15 September 1992)

ABSTRACT

For 10 regions in southwestern Europe, a comparison has been made between the surface-wave and P-wave tomography results available in the literature. Starting from the P-wave models inferred by P-wave tomography, theoretical phase velocities have been computed adjusting the ratio between P-wave and S-wave velocities in order to simultaneously fit the observed Rayleigh-wave phase velocities. The V_P/V_S ratio is an important variable that can be used to investigate the nature of variations in the propagation velocity of seismic waves in the Earth's interior. More specifically, it can be used to discriminate between thermal and compositional influences on the velocities of seismic waves. In this sense, the largest value in the distribution of the V_P/V_S ratio that we have obtained in the modelling is associated with a specific region in north-central Italy where the presence of fluids at crustal level is well known.

1. Introduction

Knowledge of the elastic parameters of the crust and the upper mantle represents a very important tool both for an understanding and the modelling of geodynamical processes in the lithosphere. In recent years, several tomographic methods have been proposed for the interpretation of seismological measurements in tectonically complex areas.

In the Mediterranean region, tomographic methods have been applied to P-waves (e.g. Spakman, 1991; Babuška and Plomerová, 1991) and surface waves (e.g. Panza et al., 1980; Snieder, 1988; Yanovskaya et al., 1990): a comparison of the results obtained with the two tomographic methods can be a powerful tool for the assessment of the V_P/V_S ratio. This can be very useful in regions where the presence of fluids in non-compacted sediments or highly fractured rocks has to be detected (O'Connel and Budianski, 1976).

2. Data

Phase velocity distribution maps, obtained by means of surface-wave tomography (e.g. Yanovskaya et al., 1990) have been considered at the periods of $T = 25$ s, $T = 50$ s and $T = 80$ s These periods are suitable for the resolution of the average Moho depth, and of the subMoho elastic properties, if a simple parametrization is used for the first, say, 200 km of structure (Knopoff and Panza, 1977).

At the period of 25 s (Fig. 1(a)) there is a quite pronounced and broad minimum affecting most of Italy and Corsica. The absolute minimum (3.55 km s^{-1}) is located near the Tyrrhenian side of north-central Italy and is related to a slow and thinned lithosphere (about 50 km) overlying low-velocity material from the asthenosphere, which extends down to a depth of about 70 km

* Corresponding author.

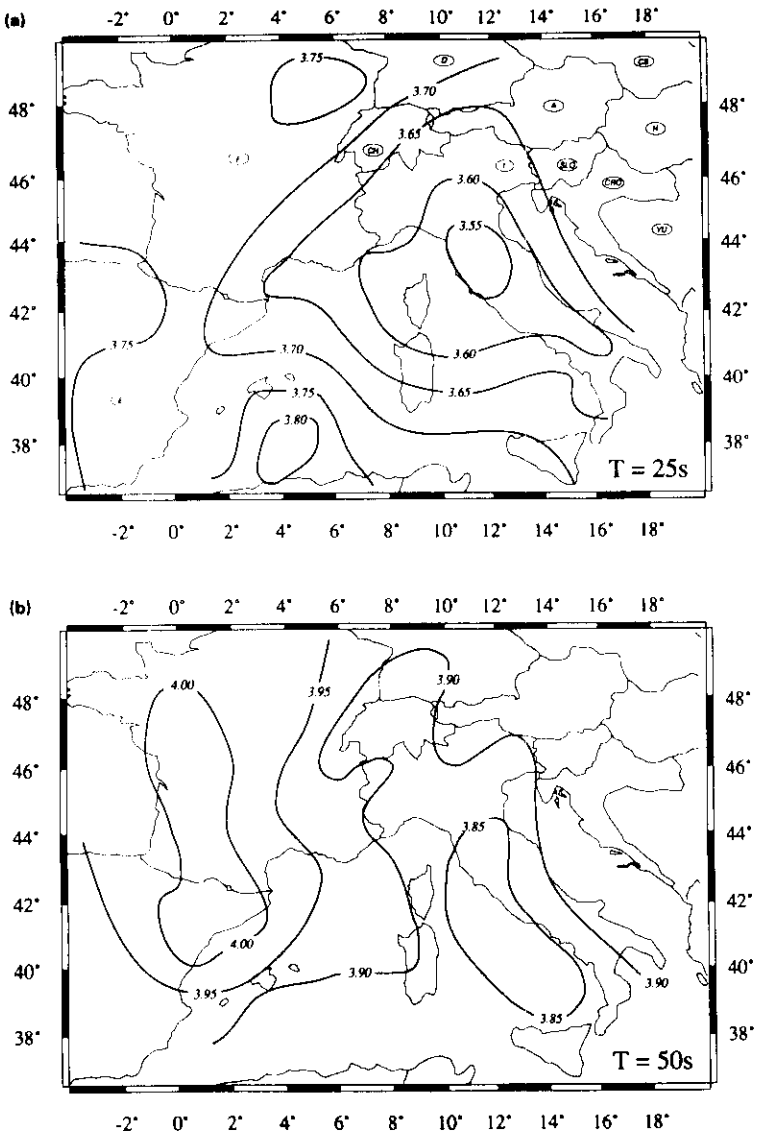

Fig. 1. Maps of phase velocities of Rayleigh waves in Western Europe: (a) $T = 25$ s, (b) $T = 50$ s (after Yanovskaya et al. (1990)). In (a) nations are indicated by their international acronyms.

(Calcagnile and Panza, 1981). The uplift of the asthenosphere is also in agreement with the high heat-flow values measured in that area (Della Vedova et al., 1991).

At the period of 50 s (Fig. 1(b)) most of the Italian peninsula is still affected by the broad minimum, but there is no evidence of an absolute minimum near the Tyrrhenian side of North Central Italy. In this area, the large increment of the phase velocity from 25 s to 50 s has been interpreted as due to the presence of fast lithospheric roots in the depth range 70–200 km (Calcagnile and Panza, 1981; Panza et al., 1982; Suhadolc and Panza, 1988). The existence of a high-velocity body has been also qualitatively confirmed by Babuška and Plomerová (1991) on the basis of the inversion of teleseismic P-wave arrivals. In Switzerland and southern Germany the relatively low-phase velocity found can be associated with the Central European rift system, characterized by a thinned lithosphere and low sublid S-wave velocities (Panza et al., 1980).

No map is given for the period of 80 s, since the variations in the Rayleigh-wave phase velocity distribution do not generally exceed the noise level, as already pointed out by Yanovskaya et al. (1990). At this period, a value of 4.00 km s^{-1} can be taken as representative of the whole area under investigation.

For the same area, the results of P-wave tomography obtained by Spakman (1991) are available along several profiles. Spakman (1991) gives results in the form of perturbations of the reference Jeffreys–Bullen (J–B) model (Bullen, 1979) used to compute the expected travel times.

3. Method and computations

To compare the results of surface-wave tomography (Yanovskaya et al., 1990) with the models given by P-wave tomography (Spakman, 1991), we have computed the phase velocities of the fundamental Rayleigh mode (Panza, 1985) for the 10

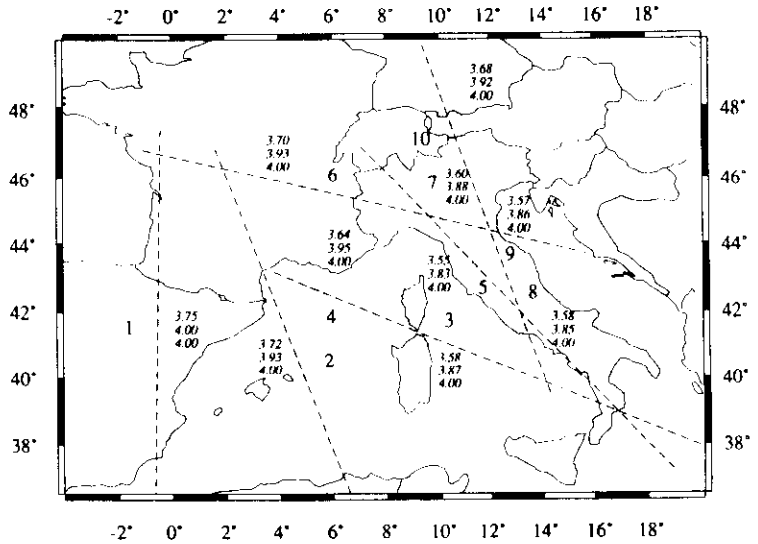

Fig. 2. Map showing the 10 regions for which a comparison has been made between surface-wave and P-wave tomography results. Dashed lines refer to the mantle sections given by Spakman (1991) which have been used in this paper. Close to each region the Rayleigh-wave phase velocities used in this study are given. From top to bottom: $T = 25$ s, $T = 50$ s, $T = 80$ s.

TABLE 1

Average crustal model assumed for the 10 regions considered

No.	Water	Solid	
	h (km)	h_c (km)	V_P (km s^{-1})
1	-	35	6.35
2	2.50	13	4.90
3	0.50	30	6.10
4	2.00	20	5.00
5	-	25	6.10
6	-	30	6.10
7	-	35	6.00
8	-	40	6.20
9	-	35	6.10
10	-	35	6.20

For the solid layers, a density of 2.6 g cm^{-3} was considered; h_c is the crustal thickness and No. is the region identification number.

regions shown in Fig. 2. We have selected these 10 regions in such a way that, on the basis of P-wave tomography, the approximation with one-dimensional layered models is acceptable.

The representative crustal models (Table 1) have been determined from the available DSS data (e.g. Mostaanpour, 1984; Buness et al., 1990; De Voogt et al., 1993) whereas for the upper mantle, the P-wave velocity distribution given by P-wave tomography has been used.

A flow chart describing the procedure adopted for the comparison is given in Fig. 3.

To compute the phase velocities of Rayleigh waves, to be compared with the values deduced from surface-wave tomography, the values of the density and of the S-wave velocities are necessary. In the crust an average density equal to 2.6 g cm^{-3} has been chosen, whereas in the mantle the density distribution of the Jeffreys–Bullen model, used by Spakman (1991) as a reference model, has been assumed. For the first set of computations, the crustal S-wave velocities have been obtained from P-wave velocities in the hypothesis of Poissonian solid. In the mantle, the distribution of the ratio between P- and S-wave velocities (V_P/V_S) given in the Jeffreys–Bullen model has been assumed. The Rayleigh-wave phase velocities computed for these starting models, shown in Fig. 4, are given in Table 2. For the same 10 regions, the Rayleigh-wave phase velocities obtained from surface-wave tomography are listed in Table 3.

It can be seen that only in region 4, without any adjustment of the initial parameters, the dispersion values obtained from surface-wave tomography are fitted within the average experimental error, about 0.06 km s^{-1}, with which phase velocities can be actually determined (e.g. Biswas and Knopoff, 1974). In the other regions, to obtain an agreement within the experimental errors the V_P/V_S value must be modified. We decided to keep as a reference the P-wave velocity distribution obtained by P-wave tomography. Therefore, if the computed phase velocities are exceeding the surface-wave tomography estimates, the V_P/V_S ratio is increased with respect to the starting models. In the opposite situation the V_P/V_S value must be decreased. The depth

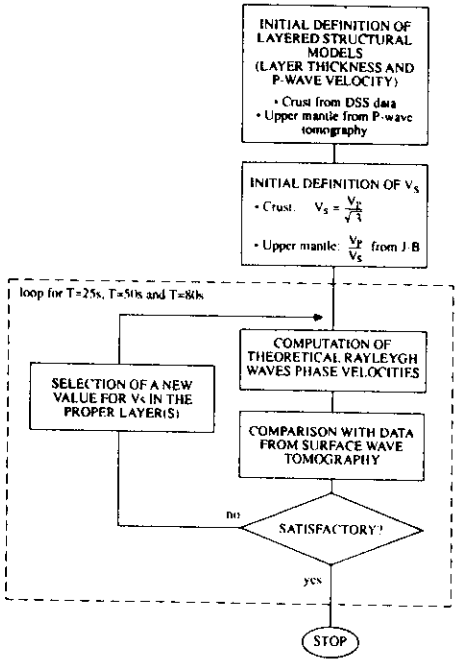

Fig. 3. Flow chart of the procedure followed for the comparison of the two tomographic data sets.

range where these variations are applied is of course controlled by the extent of the discrepancies at the different periods. As a result, a new distribution of V_S with depth is obtained.

The size of the structural details given by P-wave tomography (see Fig. 4) is much smaller than the resolution allowed by surface-wave tomography. For this reason the perturbations to

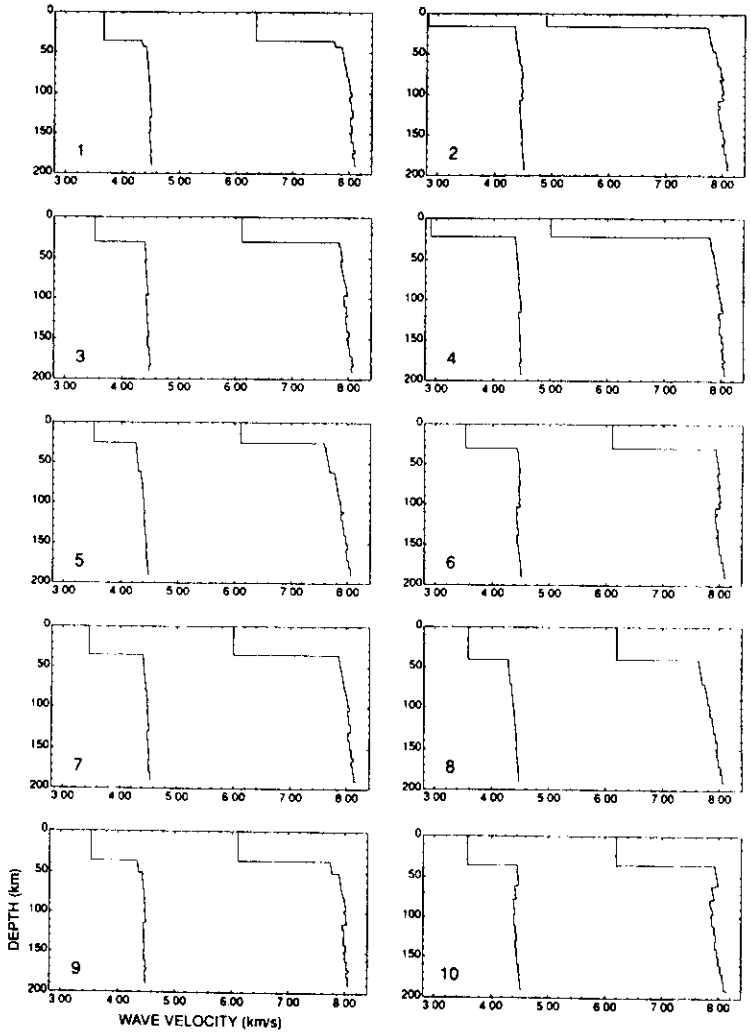

Fig. 4. Starting velocity models used to compute the theoretical Rayleigh-waves phase velocities given in Table 2.

the V_P/V_S values have been applied considering a simplified model made up of few layers (dotted lines in Fig. 5). The uppermost layer is representative of the crust, and the remaining two to three layers are used to parametrize the upper mantle (Fig. 5). Density distribution has not been modified since its influence on surface-wave propagation is negligible compared with the influence of P- and S-wave velocities.

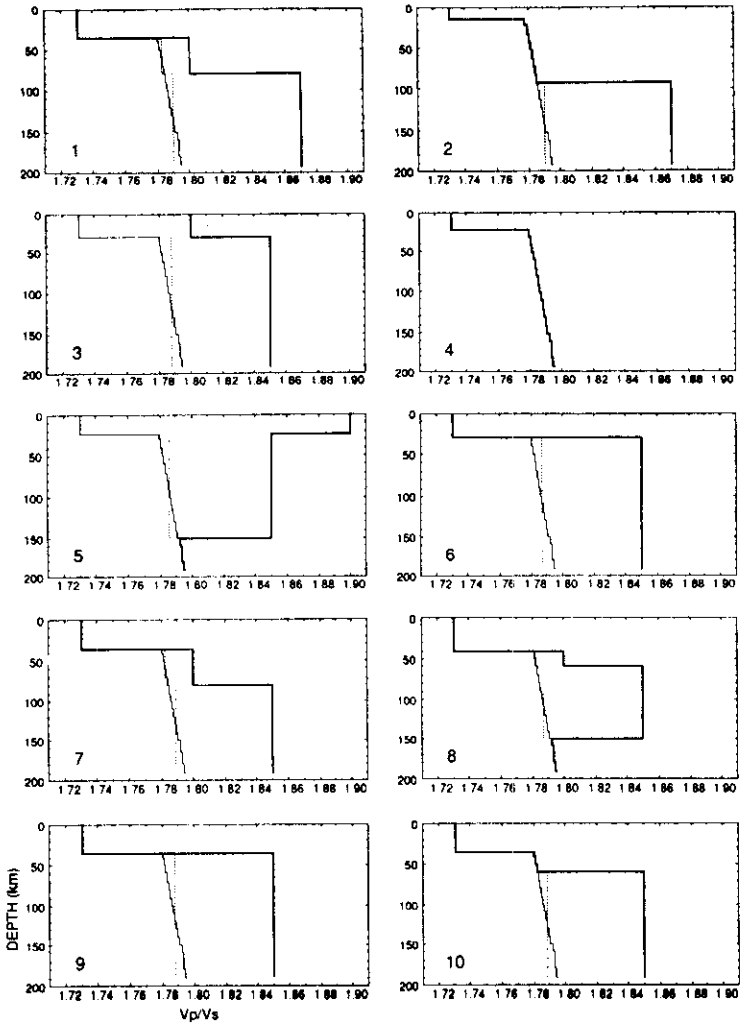

Fig. 5. V_P/V_S distribution with depth. Thin lines correspond to the initial models shown in Fig. 4. Dotted lines represent the used discretization of the initial distribution, consistent with the resolving power of surface-waves. Thick lines indicate the distribution necessary to explain simultaneously the results given by P-wave and surface-wave tomography.

TABLE 2

Rayleigh-wave phase velocities (km s^{-1}) computed for the starting models of Fig. 4

No.	Theoretical phase velocities		
	$T = 25$ s	$T = 50$ s	$T = 80$ s
1	3.76	4.04	4.15
2	3.77	3.97	4.10
3	3.75	4.00	4.11
4	3.62	3.92	4.06
5	3.78	3.97	4.09
6	3.78	4.03	4.12
7	3.61	3.99	4.12
8	3.57	3.93	4.07
9	3.64	3.99	4.11
10	3.71	4.00	4.12

No. is the region identification number.

The short-period data (25 s), which are particularly sensitive to crustal properties, are reproduced in most of the regions without any adjustment of the V_P/V_S ratio, and only in regions 3 and 5 are high ($1.8 \div 1.9$) V_P/V_S values in the crust required to fit the data.

Rayleigh waves with longer periods (50 s and 80 s) sample the upper mantle. Therefore, when necessary, to get the required agreement between observed and computed values the V_P/V_S distribution given by the Jeffreys–Bullen model must be modified. An overall good agreement between the theoretical phase velocities (Table 4) and the values obtained from surface-wave tomography is obtained assuming in the upper mantle (down to a depth of 200 km) V_P/V_S values in the range $1.80 \div 1.87$ (Fig. 5). In fact, using the V_P/V_S distribution shown in Fig. 5 (thick lines), the differences between the dispersion values obtained from surface-wave tomography and from theoretical computations are within ± 0.06 km s^{-1}, which can be considered a representative value for the experimental error affecting phase velocity measurements (Biswas and Knopoff, 1974).

TABLE 3

Rayleigh-wave phase velocity values (km s^{-1}) for the 10 regions considered (see Fig. 2)

No.	Surface-waves tomography		
	$T = 25$ s	$T = 50$ s	$T = 80$ s
1	3.75	4.00	4.00
2	3.72	3.93	4.00
3	3.58	3.87	4.00
4	3.64	3.95	4.00
5	3.55	3.83	4.00
6	3.70	3.93	4.00
7	3.60	3.88	4.00
8	3.58	3.85	4.00
9	3.57	3.86	4.00
10	3.68	3.92	4.00

No. is the region identification number. The dispersion values were derived from Yanovskaya et al. (1990).

TABLE 4

Theoretical values of Rayleigh-wave phase velocities (km s^{-1}) computed using the P-wave velocity model of Fig. 4 and the S-wave velocity model obtained from it adopting the V_P/V_S distribution of Fig. 5

No.	Theoretical phase velocities		
	$T = 25$ s	$T = 50$ s	$T = 80$ s
1	3.74	3.95	4.05
2	3.76	3.91	4.01
3	3.62	3.89	4.01
4	3.62	3.92	4.06
5	3.61	3.85	4.00
6	3.70	3.92	4.03
7	3.59	3.92	4.04
8	3.55	3.86	4.01
9	3.59	3.89	4.02
10	3.69	3.92	4.03

No. is the region identification number.

4. Discussion and conclusions

The purpose of this work is to find out whether reasonable values of the V_P/V_S ratio are compatible with the results given by P-wave and surface-wave tomography. We do not intend to perform a systematic search for possible values, so we have used a trial-and-error procedure rather than a linear inversion.

A major problem we have encountered is the absence of error bars associated with published

tomographic data, but we can assume that errors are at least comparable with the smallest details given in the maps. Therefore, our results about the V_P/V_S ratio have only the meaning of average values and indicate the gross three-dimensional variation of the ratio. The significance of small variations of V_P/V_S can be hardly addressed at present, and only variations of several per cent contain real information.

The regional variations of the distribution with depth of V_P/V_S deduced in our analysis indicate different physical conditions in the crust and in the upper mantle, even if we cannot completely exclude the presence of systematic errors in the body-wave and/or in the surface-wave data sets. The presence of sytematic errors, however, could only influence the absolute value of the retrieved V_P/V_S ratios, but relative discrepancies in the results obtained for the analysed regions are anyway meaningful. This is particularly evident in the case of the adjacent areas 5 and 9, where the retrieved V_P/V_S distributions are very different in the crust, well in agreement with the different geological settings of the two neighbouring regions.

At crustal level, the very high value of V_P/V_S in region 5, which is necessary to explain the relevant minimum in the observed phase velocity map at 25 s, is well consistent with the large thermal perturbation associated with the tensional tectonic regime in that area (Della Vedova et al., 1991). The presence of ascending deep mantle fluids reaching the crust, responsible for the anomaly, is confirmed by magmatologic studies (e.g. Locardi, 1986), and actually region 5 contains also the geothermal area of Larderello, where hot fluids are reaching the surface.

In the upper mantle, as a general feature, the V_P/V_S values obtained (Fig. 5) are larger than in the reference Jeffreys–Bullen model. This fact may possibly indicate the presence of some bias associated with the choice of the reference model used in P-wave tomography.

For the asthenosphere, the V_P/V_S values obtained in this paper are in good agreement with the values estimated by Panza et al. (1980) comparing their results based on surface-wave dispersion measurements with the P-wave velocities given by Bistricsany (1974), who analysed first arrivals from shallow-focus earthquakes.

In Central Europe, where the coverage of the profiles used in surface-wave tomography is sufficiently good, it has been noted by Yanovskaya et al. (1990) that Rayleigh-wave phase velocities show a dependence on the azimuth of the profile along which they are measured. A possible interpretation in terms of anisotropy was suggested. As a test, they introduced a correction for anisotropy in their tomographic algorithm, but the corrected patterns of lateral phase velocity distribution just slightly differ from the ones obtained for the isotropic model. Therefore, it looks as though like anisotropy plays just a secondary role and that different phase velocities along the different profiles can be well explained in terms of wave propagation in laterally heterogeneous media. In principle, both lateral heterogeneities and anisotropy should be taken into account, but with the presently available dispersion data for the area, it seems impossible to separate the two effects.

It has been noted in several cases (e.g. Cara et al., 1980; Wielandt et al., 1987) that models explaining Rayleigh-wave dispersion curves are incompatible with Love-wave phase velocity measurements. To explain this inconsistency in terms of anisotropy, a strongly coherent orientation of minerals is required along the different paths. This is not likely to happen in continental areas, where the geological and tectonic processes very often lead to a non-homogeneous distribution of rocks and to rather complex structures, for which it is difficult to imagine any large-scale coherency. In such a case, it is very difficult to separate the effects of anisotropy from those of lateral heterogeneities just on the basis of seismic tomography, and also geological and petrological data have to be taken into account.

In this paper, modifying the reference V_P/V_S distribution of the Jeffreys–Bullen model, we have simultaneously satisfied P-wave and Rayleigh-wave observations at different periods. Therefore, within the resolving power of the available data for the investigated region, it seems unnecessary to invoke the presence of relevant anisotropic phenomena in the upper mantle.

The perturbation of the V_P/V_S distribution should be used in the case where structural models explaining the observed Rayleigh-wave dispersion curves are not compatible with Love-wave data. If, after the V_P/V_S perturbation has been applied to make Love- and Rayleigh-wave data sets consistent, the adjusted models are also compatible with available images given by P-wave tomography, then the conclusion can be drawn that anisotropy is not relevant in the region investigated. On the contrary, anomalies that cannot be explained through a perturbation of the V_P/V_S ratio, very probably must be interpreted in terms of anisotropy.

Acknowledgements

The authors wish to thank, for their partial financial support, the Ministero Università e Ricerca Scientifica e Tecnologica (60% and 40% funds), and the Consiglio Nazionale delle Ricerche (GNDT, contracts 89.02015.54 and 90.01007.54), Rome. This is a contribution to the ILP Task Group II-4.

References

Babuška, V. and Plomerová, J., 1991. Tomographic studies of the upper mantle beneath the Italian region. Terra Nova, 2: 569–576.

Bistricsany, E., 1974. The depth of the LVL in Europe and in some adjacent regions. Geofizikai Közlemenyek, 22: 61–63.

Biswas, N.N. and Knopoff, L., 1974. Structure of the upper mantle under the United States from the dispersion of Rayleigh waves. Geophys. J. R. Astron. Soc., 36: 515–539.

Bullen, K.E., 1979. An Introduction to the Theory of Seismology, 3rd eds. Cambridge University, Cambridge, p. 223.

Buness, H., Giese, P., Hirn, A., Nadir, S. and Scarascia, S., 1990. Crustal structure derived from seismic refraction between the Southern Alps and the Ligurian Sea. In: R. Freeman and St. Mueller (Editors), Proc. Sixth Workshop on the European Geotraverse (EGT) Project, Data Compilations and Synoptic Interpretation, European Science Foundation, Strasbourg, pp. 165–168.

Calcagnile, G. and Panza, G.F., 1981. The main characteristics of the lithosphere–asthenosphere system in Italy and surrounding regions. Pure Appl. Geophys., 119: 865–879.

Cara, M., Nercessian, A. and Nolet, G., 1980. New inferences from higher mode data of the Pacific revisited. Geophys. Res. Lett., 15: 205–208.

Della Vedova, B., Marson, I., Panza, G.F. and Suhadolc, P., 1991. Upper mantle properties of the Tuscan–Tyrrhenian area: a framework for its recent tectonic evolution. In: R. Freeman, M. Huch and St. Mueller (Editors), The European GeoTraverse, Part 7. Tectonophysics, 195: 311–318.

De Voogt, B., et al., 1993. First deep seismic reflection transect from the Gulf of Lions to Sardinia (ECORS–CROP profiles in Western Mediterranean). Proc. Bayreuth Conf., 4th Int. Symp. on Deep Seismic Reflection Profiling of the Continental Lithosphere. AGU Geodyn. Ser., in press.

Knopoff, L. and Panza, G.F., 1977. Resolution of upper mantle structure using higher modes of Rayleigh waves. Ann. Geofis., 30: 491–505.

Locardi, E., 1986. Tyrrhenian volcanic arcs: volcano-tectonics, petrogenesis and economic aspects. In: F.-C. Wezel (Editor), The Origin of Arcs. Elsevier Science, Amsterdam, pp. 351–373.

Mostaanpour, M.M., 1984. Einheitliche Auswertung krustenseismischer Daten in Westeuropa. Darstellung von Krusten-parametern und Laufzeitanomalien. Berliner Geowissenschaftlichen Abhandlungen, D 188, Verlag von Dietrich Reimer, Berlin, Germany.

O'Connel, R. and Budianski, B., 1976. Seismic velocities in dry and saturated cracked solid. J. Geophys. Res., 79: 5413–5426.

Panza, G.F., 1985. Synthetic seismograms: The Rayleigh waves modal summation. J. Geophys., 58: 125–145.

Panza, G.F., Mueller, St. and Calcagnile, G., 1980. The gross features of the lithosphere–asthenosphere system in Europe from seismic surface waves and body waves. Pure Appl. Geophys. 118: 1209–1213.

Panza, G.F., Mueller, S., Calcagnile, G. and Knopoff, L., 1982. Delineation of the north central Italian upper mantle anomaly. Nature, 296: 238–239.

Snieder, R., 1988. Large-scale waveform inversions of surface waves for lateral heterogeneity—2. Application to surface waves in Europe and the Mediterranean. J. Geophys. Res., 93: 12067–12080.

Spakman, W., 1991. Tomographic images of the upper mantle below Central Europe and the Mediterranean. Terra Nova, 2: 542–553.

Suhadolc, P. and Panza, G.F., 1988. The European–African collision and its effects on the lithosphere–asthenosphere system. Tectonophysics, 146: 59–66.

Wielandt, E., Sigg, A., Plesinger, A. and Horalek J., 1987. Deep structure of the Bohemian massif from phase velocities of Rayleigh and Love waves. Studia Geophys. Geod., 31: 121–127.

Yanovskaya, T.B., Panza, G.F., Ditmar, P.G., Suhadolc, P. and Mueller, St., 1990. Structural heterogeneous and anisotropy based on 2-D phase velocity patterns of Rayleigh waves in Western Europe. Atti Accad. Naz. Lincei, 1: 127–135.